# Screening of Slow Speed Marine Diesel Propulsion Shafting Design Space

*Gojko MAGAZINOVIĆ*

Fakultet elektrotehnike, strojarstva i brodogradnje Sveučilišta u Splitu (Faculty of Electrical Engineering, Mechanical Engineering and Naval Architecture, University of Split),
Ruđera Boškovića bb,
HR - 21000 Split, **Republic of Croatia**

gmag@fesb.hr

Original scientific paper

In this paper a systematic exploration of a typical two-stroke slow speed marine diesel propulsion shafting design space is performed. First, a set of the four most influential design parameters is defined, consisting of shafting stiffness, propeller, turning wheel and tuning wheel mass moments of inertia. Then, a full set of 625 design points is defined. For each design point a complete torsional vibration analysis has been performed, and the three most significant results were collected. These are the first torsional natural frequency, crankshaft peak torque and shafting peak torque. Finally, the results are presented in three series of response surface diagrams. Furthermore, the ability of each system parameter to change the system response is analysed by using Saaty's priority theory. The presented results provide better insight into the propulsion system torsional vibration behaviour and encourage designers to achieve a desired design solution already in the preliminary design phase. Although the key findings are related to the specific diesel engine only, it is believed that the presented behaviour is quite general and hence qualitatively applicable to a much broader range of the two-stroke slow speed diesel propulsion plants.

**Pretraživanje projektnoga prostora voda vratila sporohodnih brodskih dizelskih porivnih postrojenja**

Izvornoznanstveni članak

U ovom radu je izvršeno sustavno pretraživanje projektnoga prostora voda vratila tipičnoga dvotaktnog sporohodnog brodskog dizelskog porivnog postrojenja. Prvo je određen skup četiriju najutjecajnijih projektnih parametara koji tvore krutost voda vratila i momenti tromosti brodskoga vijka, zamašnjaka i pramčanoga zamašnjaka. Nakon toga je određen skup od 625 projektnih točaka. Za svaku projektnu točku su izvršene cjelovite analize torzijskih vibracija i prikupljene vrijednosti triju najznačajnijih rezultata. To su prva torzijska prirodna frekvencija, vršni moment u koljenastom vratilu i vršni moment u vodu vratila. Konačno, rezultati su prikazani u tri niza dijagrama odzivnih ploha. Osim toga, uz primjenu Saatyjeve teorije prednosti, analiziran je i kvantificiran upliv svakoga od parametara na odziv sustava. Prikazani rezultati omogućuju bolji uvid u držanje torzijskih vibracija porivnih postrojenja i potiču projektante da postignu željeno projektno rješenje već u početnoj fazi projekta. Iako se ključni nalazi odnose isključivo na određeni dizelski motor, vjeruje se kako je prikazano držanje dovoljno općenito i zato kvalitativno primjenljivo na znatno šire područje dvotaktnih sporohodnih dizelskih porivnih sustava.

## 1. Introduction

Design space could be defined as a space of possible design solutions. Such space is in general unbounded and infinite. On the other hand, feasible design space corresponds to the space of feasible design solutions. Feasible design space is generally bounded, but also infinite. The designer's task is to provide a feasible design solution that best meets imposed design intent, usually defined by a set of objectives and constraints.

The shafting arrangements of the majority ocean-going merchant vessels are very similar [1]. In general, they consist of a two-stroke slow speed diesel engine, direct coupled intermediate shaft, propeller shaft, and a fixed-pitch propeller, as depicted in Figure 1. The propulsion shafting's main purpose is reliable propelling of the vessel during its whole lifecycle. Therefore, the propulsion shafting system design must be accomplished with the utmost care, due to its importance for the vessel's overall performance.

Literature devoted to the field of marine propulsion shafting system design is surprisingly sparse. Probably the most complete source is the work of Long [1]. There are also some vintage references [2-3] of doubtful

**Symbols/Oznake**

| | | | | |
|---|---|---|---|---|
| $\mathbf{C}$ | - damping matrix<br>- matrica prigušenja | | $T_c$ | - crankshaft peak torque, N·m<br>- vršni vibracijski moment u koljenastom vratilu |
| $d$ | - shaft element diameter, m<br>- promjer dionice vratila | | $T_s$ | - shafting peak torque, N·m<br>- vršni vibracijski moment u vodu vratila |
| $f$ | - first torsional natural frequency, min$^{-1}$ (CPM)<br>- prva prirodna torzijska frekvencija | | $\mathbf{v}$ | - eigenvector<br>- svojstveni vektor |
| $\mathbf{f}$ | - load vector<br>- vektor opterećenja | | $w$ | - weight factor<br>- težinski faktor |
| $F$ | - complex excitation torque amplitude, N·m<br>- amplituda kompleksnoga pobudnog momenta | | $z$ | - number of engine cylinders<br>- broj cilindara motora |
| $\Delta f$ | - response change<br>- promjena odziva | | $\overline{\Delta}$ | - average response change<br>- prosječna promjena odziva |
| $\mathbf{J}$ | - inertia matrix<br>- matrica tromosti | | $\theta_i$ | - shaft element angular displacement, rad<br>- kutni pomak dionice vratila |
| $J_F$ | - turning wheel inertia, kg·m$^2$<br>- tromost zamašnjaka | | $\boldsymbol{\theta}$ | - angular displacement vector<br>- vektor kutnih pomaka |
| $J_P$ | - propeller inertia, kg·m$^2$<br>- tromost brodskoga vijka | | $\dot{\boldsymbol{\theta}}$ | - angular velocity vector<br>- vektor kutnih brzina |
| $J_T$ | - tuning wheel inertia, kg·m$^2$<br>- tromost pramčanoga zamašnjaka | | $\ddot{\boldsymbol{\theta}}$ | - angular acceleration vector<br>- vektor kutnih ubrzanja |
| $k_t$ | - shaft torsional stiffness, N·m/rad<br>- torzijska krutost vratila | | $\Theta$ | - complex angular displacement amplitude, rad<br>- amplituda kompleksnoga kutnog pomaka |
| $\mathbf{K}$ | - stiffness matrix<br>- matrica krutosti | | $\lambda$ | - eigenvalue<br>- svojstvena vrijednost |
| $m$ | - number of shaft elements<br>- broj dionica voda vratila | | $\tau_i$ | - vibration torsional stress, N/m$^2$<br>- vibracijsko torzijsko naprezanje |
| $n_c$ | - critical shaft speed, min$^{-1}$<br>- kritična brzina vrtnje vratila | | $\tau_1$ | - stress limit for engine continuous running, N/m$^2$<br>- dopušteno torzijsko naprezanje za trajni rad motora |
| $N_p$ | - number of design points<br>- broj projektnih točaka | | $\tau_2$ | - stress limit for engine transient operation, N/m$^2$<br>- dopušteno torzijsko naprezanje tijekom prolaznih pojava |
| $N_s$ | - number of data samples<br>- broj uzoraka | | $\Omega$ | - excitation frequency, rad/s<br>- frekvencija pobude |
| $r$ | - comparison ratio<br>- omjer uspoređivanih veličina | | | |
| $\mathbf{R}$ | - comparison matrix<br>- matrica usporedbi | | **Subscripts / Donji indeksi** | |
| $t$ | - time, s<br>- vrijeme | | i | - shaft element index; first parameter considered<br>- redni broj dionice voda vratila; prvi promatrani parametar |
| $T_i$ | - vibration torque amplitude, N·m<br>- amplituda vibracijskoga momenta | | j | - second parameter considered<br>- drugi promatrani parametar |
| | | | k | - vibration response considered<br>- promatrani vibracijski odziv |

applicability, due to changes and progress achieved in the field. Of the more recent publications, two of them deserve more attention from the practical point of view. The first one [4] introduces the concepts of flexible and stiff shafting, with the specific design approaches based on them. The second paper [5] stresses the importance of fatigue considerations in the shafting design and provide means for a more thorough shafting evaluation. When practical solutions of the specific design tasks

are concerned, some directions could be found in Magazinović [6-8]. However it should be noted that nearly all contemporary sources deal with the torsional vibration aspects of the shafting design only, while its complete design scope is actually much wider − for example, the issue of propulsion shafting alignment [9] deserves major attention. This seemingly strange fact could be explained as follows. The propulsion shafting is a complex system exposed to various static and dynamic

loads that require a multidisciplinary design approach. Moreover, its design is a subject of several regulatory means. However, it could be shown that the torsional vibration behaviour is the most influential propulsion shafting design aspect. Therefore, the shafting satisfactory torsional vibration behaviour becomes the subject of primary design importance.
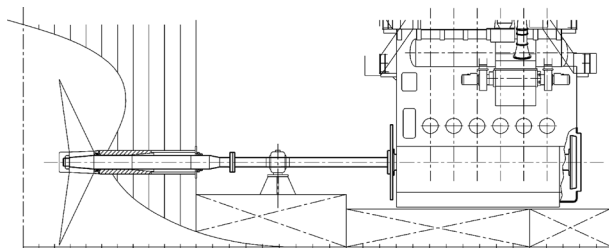


**Figure 1.** Typical two-stroke low speed marine diesel propulsion plant shafting arrangement

**Slika 1.** Tipična izvedba voda vratila dvotaktnoga sporohodnog brodskog dizelskog porivnog postrojenja

Design space analysis has recently become a field of increased research interest [10-12]. In this paper a concept of the design space screening is proposed and utilized as a design tool. Visualization of the response surfaces enables a more thorough insight into the propulsion system torsional vibration behaviour and encourages designers to achieve a desired design solution already in the preliminary design phase.

This paper is organised as follows. In Section 2 a brief overview of the propulsion shafting torsional vibration analysis is given. The analysed design space is defined and discussed in Section 3, and the results of the performed analyses are provided in Section 4. Some points which require more explanation are discussed in Section 5. Finally, in Section 6, the key findings of the present study are summarized.

## 2. Torsional vibration response

There is a great number of approaches to shafting torsional vibration analysis, from early works based on Holzer's tabulation [13-15], to more recent applications of numerical modal analysis techniques [16-19]. However, all these methods share much in common: the continuous shafting system needs to be divided in the so-called lumped mass system where, after applying equations of motion, one evaluates natural frequencies, accompanied mode shapes and, in the case of forced torsional vibrations, angular displacements of all masses. After that, it is straightforward to determine vibration torques and stresses.

The above procedure is mathematically summarized as follows. Equations of motion of the lumped mass system could be gathered in a common matrix equation:

$$\mathbf{J}\ddot{\boldsymbol{\theta}} + \mathbf{C}\dot{\boldsymbol{\theta}} + \mathbf{K}\boldsymbol{\theta} = \mathbf{f} , \tag{1}$$

where $\mathbf{J}$ is the diagonal inertia matrix, $\mathbf{C}$ is the symmetric damping matrix, $\mathbf{K}$ is the symmetric stiffness matrix, and $\ddot{\boldsymbol{\theta}}$, $\dot{\boldsymbol{\theta}}$ and $\boldsymbol{\theta}$ are the angular acceleration, velocity and displacement vectors, respectively. On the right hand side, $\mathbf{f}$ denotes the applied load, expressed with vibration excitation vector. Equations of motion (1) represent a non-homogenous system of linear ordinary differential equations of second order with constant coefficients, where the number of equations is determined by the number of lumped masses.

Natural frequencies as well as the corresponding modes of vibration of the free undamped vibrations are the result of the eigenvalue problem [19] obtained from equation (1), when the applied load and damping matrix are both set to zero.

Forced damped torsional vibration response could be obtained in various ways. By assuming harmonic excitation:

$$f = Fe^{i\Omega t} , \tag{2}$$

and harmonic response in the form:

$$\theta = \Theta e^{i\Omega t} , \tag{3}$$

where $F$ is the complex excitation torque amplitude, $\Omega$ is the excitation frequency, $t$ is the time, and $\Theta$ is the complex angular displacement amplitude, the system of equations (1) readily transforms into a system of linear algebraic equations with complex coefficients:

$$-\Omega^2 \mathbf{J}\boldsymbol{\Theta} + i\Omega\mathbf{C}\boldsymbol{\Theta} + \mathbf{K}\boldsymbol{\Theta} = \mathbf{F} . \tag{4}$$

By solving the system of equations (4), the unknown angular displacement amplitudes and phase angles become available. Vibration torque amplitudes between the adjacent masses could then be obtained from:

$$T_i = k_{\mathrm{t},i} \cdot (\theta_{i+1} - \theta_i) , \quad i = 1, 2, \dots m , \tag{5}$$

where $k_\mathrm{t}$ is the shaft stiffness, $(\theta_{i+1} - \theta_i)$ is the amplitude of the shaft element twist, and $m$ is the number of shaft elements. Afterwards, the vibration stresses could be easily determined from:

$$\tau_i = \frac{16 \cdot T_i}{d_i^3 \cdot \pi} , \qquad i = 1, 2, \dots m , \tag{6}$$

where $d$ is the shaft element diameter.

## 3. Design space

The propulsion shafting design space is generally a highly dimensional, multi-axis system. Since such multidimensional systems are highly elaborate for analysis, it is necessary to reduce the number of dimensions as much as possible. However, that process should be done very carefully in order to preserve the intrinsic behaviour of the system.

Shafting dimensions constitute an array of the shaft section diameters and the corresponding shaft lengths. Then, depending on actual arrangement, the number of system parameters may vary from reasonably low 30, to more than 50. Since any system parameter could be seen as a specific design space axis, the dimensionality of such design space becomes prohibitively large. Fortunately, for preliminary design purposes, the complete shafting could be modelled as a two-parameter system, consisting of shafting stiffness and the corresponding mass moment of inertia. Furthermore, if the shafting mass moment of inertia is divided in two parts, and each of them is added to the adjacent propeller or turning wheel inertias, the complete shafting design could be satisfactorily modelled by a shafting stiffness only. By applying this approach, the propulsion shafting system design could be defined by as low as the four dimensional–four axis design space. Therefore, the four axes considered are the shafting stiffness, propeller mass moment of inertia, turning wheel mass moment of inertia and, when applicable, the tuning wheel mass moment of inertia. It is worth noting that the propulsion engine is not explicitly included here as an additional design space axis, since the pre-defined engine type is already assumed. This way the dimensionality of the design space is retained in four dimensions only.

For the purpose of this study a MAN B&W 6S60MC-C two-stroke slow speed diesel engine is selected as a prime mover, Table 1. It is a matured, well developed engine design, readily selected for the Panamax and Aframax-sized ocean-going vessel propulsion.

**Table 1.** Selected engine data

**Tablica 1.** Podaci izabranoga motora

| Engine type / Vrsta motora | MAN B&W 6S60MC-C7 |
|---|---|
| Maximum continuous output / Najveća trajna snaga | 13560 kW |
| Maximum continuous speed / Najveća trajna brzina vrtnje | 105 min⁻¹ |
| Number of cylinders / Broj cilindara | 6, inline / redni |
| Cylinder bore / Promjer cilindra | 600 mm |
| Stroke / Stapaj | 2400 mm |
| Firing order / Redoslijed izgaranja | 1-5-3-4-2-6 |

**Table 2.** Design space considered

**Tablica 2.** Promatrani projektni prostor

| Axis / Os | Unit / Jedinica | Lower bound / Donja granica | Upper bound / Gornja granica | Increment / Prirast |
|---|---|---|---|---|
| Shafting stiffness / Krutost vratila | MN·m/ rad | 20 | 60 | 10 |
| Propeller inertia / Tromost vijka | kg·m² | 60000 | 88000 | 7000 |
| Turning wheel inertia /Tromost zamašnjaka | kg·m² | 5000 | 22000 | 4250 |
| Tuning wheel inertia / Tromost pramčanoga zamašnjaka | kg·m² | 0 | 30000 | 7500 |

Characteristics of the screened design space are given in Table 2. The shafting stiffness encompasses a range between 20 and 60 MN·m/rad, the range that is customary referred to as a flexible shafting. The lower bound of 20 MN·m/rad roughly corresponds to a 20 m long shafting composed of the 460 mm diameter intermediate shaft and 530 mm diameter propeller shaft. On the other hand, the upper bound stiffness of 60 MN·m/rad matches a 15 m long shafting composed of the 550 mm diameter intermediate shaft and 670 mm diameter propeller shaft. These values make up the common majority of the propulsion shafting designs usually applied to the selected engine. Of course, the actual shafting lengths could be significantly different, if the other shaft diameters are considered. This axis is represented by five equidistant values, as suggested in Table 1.

The propeller mass moment of inertia axis of the proposed design space is bounded by range from 60000 to 88000 kg·m². These values are functions of the propeller hub and propeller blade design and include the effects of the entrained water [20]. Furthermore, these values also partly include the inertia effect of the propulsion shafting. As in the case of shafting stiffness, the selected range encompasses the majority of propeller designs applied to the selected propulsion engine.

The turning wheel is an obligatory feature of all propulsion engines. Therefore, it is included in the design space as a stand-alone axis. The selected range from 5000 to 22000 kg·m² encompasses the complete range of values recommended and allowed by the selected engine builders. It is worth noting that these values should also take into account the partial effect of the propulsion shafting mass moment of inertia.

The tuning wheel is an optional feature of the propulsion engine. In general, its inclusion is a consequence of the already performed torsional vibration analysis. Depending on system particulars a more desirable forced vibration response could be obtained by proper sizing of the tuning wheel. The selected tuning wheel mass moment of inertia ranges from zero to 30000 kg·m² and encompasses the whole range of recommended and allowed values by the selected engine builders. The zero mass moment of inertia implies an initial state when no tuning wheel is installed.

Since each axis includes five distinct values, the whole design space results in a full set of $N_p = 5^4 = 625$ design points.

# 4. Results

For each design point defined in the previous section a full natural and forced torsional vibration analysis has been furnished. Calculations were performed by the procedure briefly reviewed in Section 2, by the custom made computer code *TorViC v1.1* [21].

Of the great number of calculation results, only three of them from each analysis have been collected. These are the system first natural torsional frequency, the crankshaft peak vibration torque and the propulsion shafting peak vibration torque. The peak vibration torques were determined by a series of forced torsional vibration calculations performed in the engine speed range from 30 to 110 min⁻¹, with the 0,1 min⁻¹ engine speed increment.

Although only three results from each analysis were considered in this study, their practical significance is much higher. Namely, by knowing the first torsional natural frequency *f*, it is possible to estimate the system main resonance, also known as the so-called critical shaft speed $n_c$, defined as:

$$n_c = f / z, \tag{7}$$

where *z* is the number of engine cylinders. Then, by applying International Association of Classification Societies Unified Requirements [22], the barred speed range becomes readily available. On the other hand, availability of the engine crankshaft peak vibration torque enables determination of the crankshaft stress level. Similarly, the shafting peak torque enables assessment of the intermediate shaft and propeller shaft stress levels. Strictly speaking, in these two shafting elements two different torque levels exist, but their difference in the preliminary design phase of typical shafting arrangements could be neglected. Furthermore, the shafting peak torque levels provide the propeller hub as well as shrink-fit or flange connection verification. These results taken together provide sufficient information for the proper evaluation of the propulsion shafting preliminary design.

The results of this study are provided in Figures 2, 3 and 6. Figure 2 shows the relationship between the first torsional natural frequencies and the screened design space. Similarly, Figure 3 provides the relationship between the crankshaft peak vibration torques and the design space, while Figure 6 gives the corresponding relationship for the shafting peak vibration torques. Each figure comprises eight diagrams, arranged in two columns, consisting of 25 design points each, resulting in a total of 200 design points. However, the actual sum of the distinct design points is slightly lower − 168, due to the fact that some design points were already shown on other diagrams. Therefore, it follows that each figure visualizes approximately the one fourth or 27 % to be more precise, of the screened design space.

## 4.1. Natural frequency

Natural frequencies are intrinsic properties of any vibration system. When the two-stroke slow speed diesel propulsion plants are concerned, the first torsional natural frequency is the most important, while others are generally less influential, and therefore omitted from this study.

The values of the torsional first natural frequency within the screened design space, Figure 2, range between 185 and 385 cycles per minute, cpm, resulting in the critical shaft speeds range from 31 to 64 min⁻¹. The least natural frequency corresponds to the least shafting stiffness and the largest propeller, turning wheel and tuning wheel mass moments of inertia, Figure 2(g). On the contrary, the highest natural frequency corresponds to the highest shafting stiffness and the least propeller, turning wheel and tuning wheel mass moments of inertia, Figure 2(e). Such behaviour is quite expected since it strictly follows the fundamentals of vibration theory.

Figures 2(a)-(d) show a relationship between the first natural frequency and turning wheel and tuning wheel inertias. The relationship between the first natural frequency and shafting stiffness and propeller inertia is provided in Figures 2(e)-(h). Diagrams in both groups follow the same column-specific pattern. Furthermore, all response surfaces are smooth and monotone, causing all extremes to be positioned on the design space boundaries.

In order to quantify the natural frequency sensitivity with respect to the system parameters change, an average response change $\overline{\Delta}$ is introduced, defined as:

$$\overline{\Delta} = \frac{1}{N_s} \sum_{i=1}^{N_s} \Delta f_i , \tag{8}$$

where $\Delta f_i$ is the largest response change that could be obtained by any change (within the screened design space) of a system parameter concerned, and $N_s$ is the
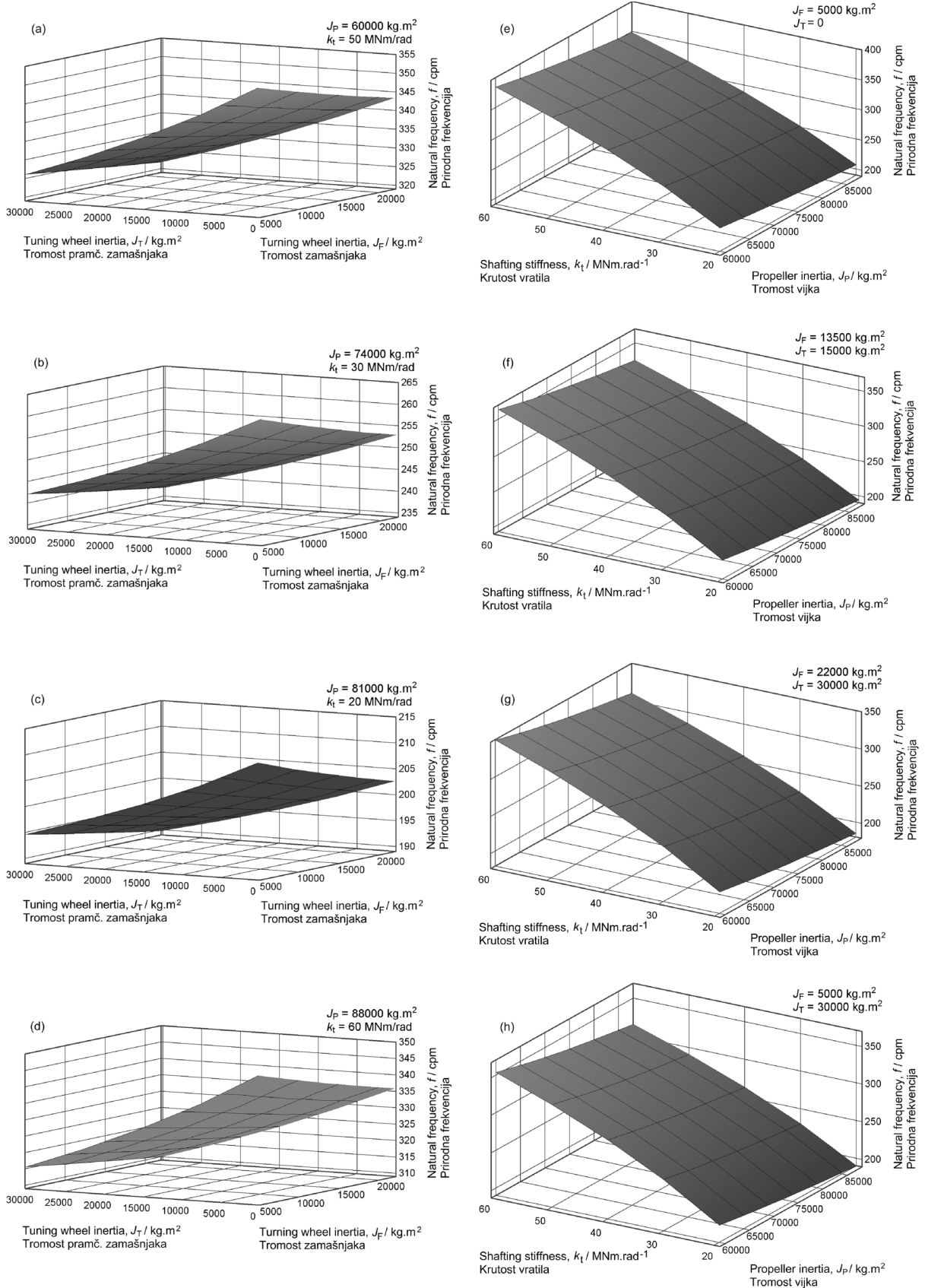
**Figure 2.** Torsional first natural frequency response surfaces

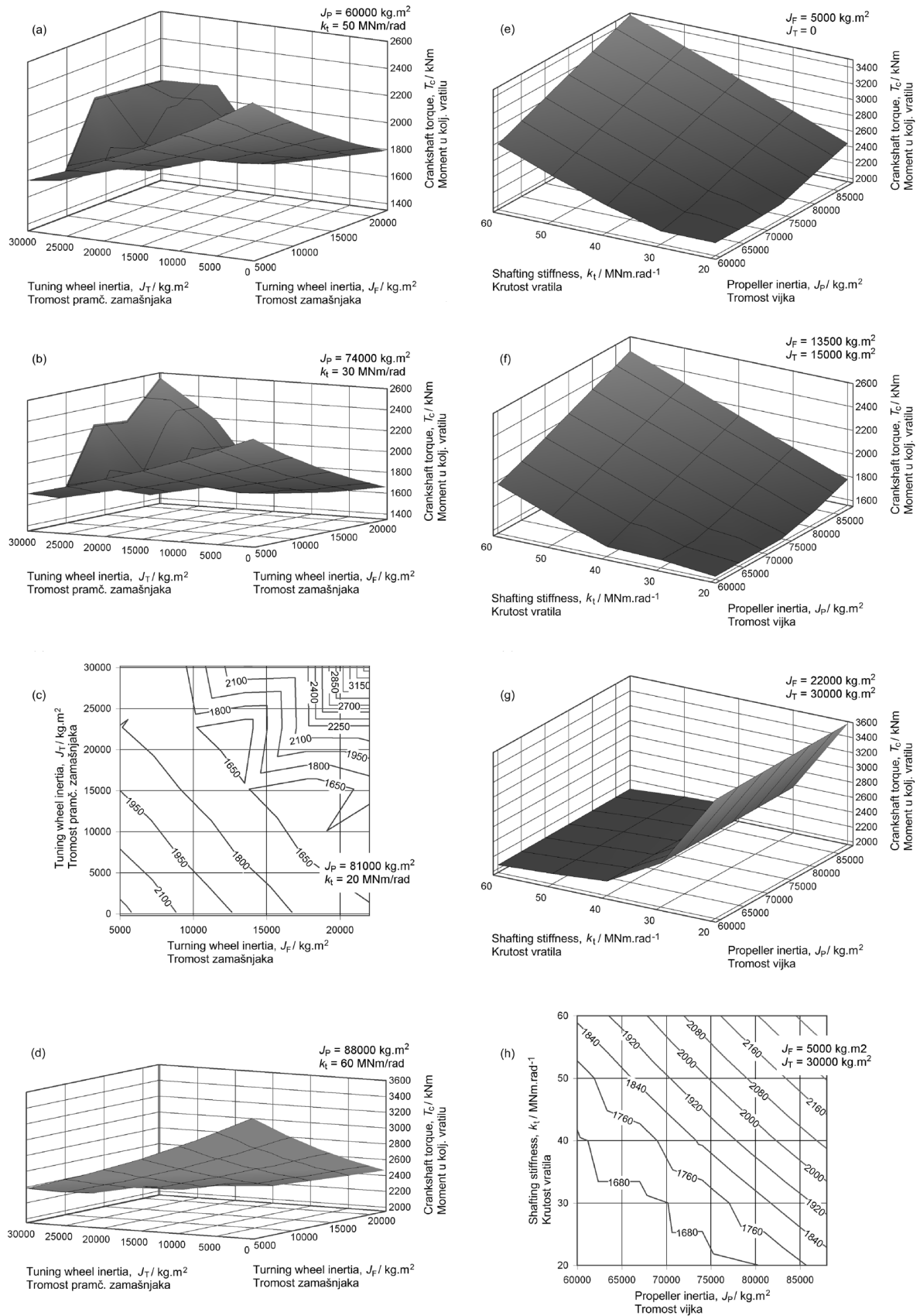**Slika 2.** Odzivne plohe prve torzijske prirodne frekvencije

**Figure 3.** Crankshaft peak torque response surfaces

**Slika 3.** Odzivne plohe vršnoga torzijskog momenta u koljenastom vratilu

number of samples. Since the summation in equation (8) is performed over the three coordinate axes, containing five points each, the total number of samples equals $N_s = 5^3 = 125$.

By applying the above procedure it could be shown that the natural frequency is the most sensitive to the shafting stiffness change ($\overline{\Delta} = 139$ cpm). On the other hand, the natural frequency is the least sensitive to the turning wheel mass moment of inertia, where a 7,4 cpm average change is found. The moderate sensitivity is found with respect to the tuning wheel ($\overline{\Delta} = 21,7$ cpm) and propeller mass moments of inertia, $\overline{\Delta} = 30,9$ cpm.

## 4.2. Crankshaft peak torque

Response surfaces of the crankshaft peak torque, Figure 3, show very interesting behaviour. In contrast to the natural frequency responses, Figure 2, the provided surfaces are neither smooth nor monotone. The minimum crankshaft peak torque found equals 1463 kN·m, while the maximum one is 3575 kN·m. The maximum crankshaft peak torque corresponds to the least shafting stiffness and the highest propeller, turning wheel and tuning wheel mass moments of inertia, Figure 3(e). Where the least crankshaft peak torque is concerned, its design point is not positioned completely on the design space boundary. Instead, even two distinct local minima are identified. Both of them correspond to the least shafting stiffness and propeller mass moment of inertia, while the turning wheel and tuning wheel inertia coordinates correspond to (13500; 22500) and (17750; 15000), respectively, as suggested in Figure 3(c).

The cause of such behaviour is a rise of the crankshaft peak torque induced by resonances other than the main. For the selected propulsion plant the main resonance is the I-node, 6th order (customary denoted as I/6) torsional critical. Other resonances are, in general, more or less negligible. However, under some circumstances, when the low stiffness shafting is connected to engines equipped with the large tuning wheels and turning wheels, the impact of other resonances could become predominant, Figure 4. This phenomenon is clearly shown in Figures 3(a)-(d), where I/3 and II/9 criticals prevail, Figures 3(a)-(c). This phenomenon is also visualised in Figures 3(f)-(g), where an abrupt change in the response surface shape is shown. The large wheels tend to isolate the engine crankshaft from the rest of the system, when the propeller loses nearly all its influence, Figure 3(g). On the contrary, in the case of a stiff shafting, the role of a propeller is not attenuated, and the impact of other resonances is nearly negligible, Figure 3(d).
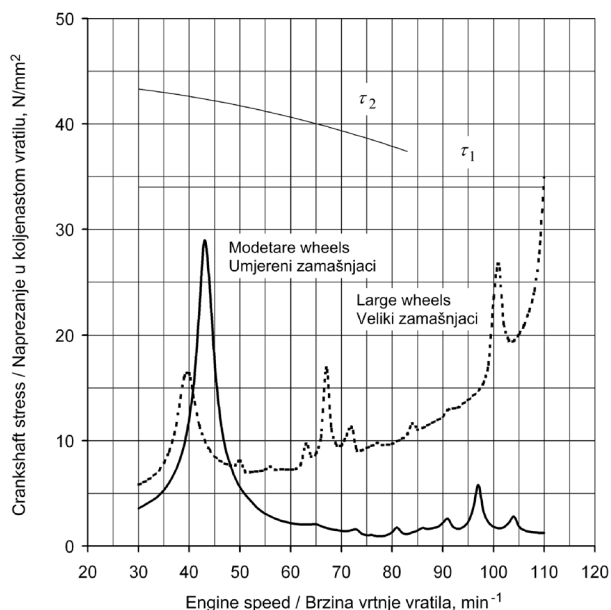


**Figure 4.** Typical crankshaft torsional vibration response
**Slika 4.** Tipični odziv torzijskih vibracija koljenastoga vratila

Figure 4 depicts the crankshaft stress levels for the two typical shafting arrangements. The first one, denoted *Moderate wheels*, has no tuning wheel at all, and the turning wheel of 10000 kg·m² mass moment of inertia is installed. The second arrangement, denoted *Large wheels*, is characterised by the largest tuning wheels and turning wheels allowed by the engine builder's specification, Table 2. Other parameters of interest are the 74000 kg·m² mass moment of inertia propeller and 30 MN·m/rad stiffness shafting. In the case of the moderate wheels, the first two torsional natural frequencies are 260 and 1454 cpm, respectively. In the case of large wheels, the corresponding natural frequency equals 237 and 1005 cpm, respectively. While the first natural frequency reduced for about 10 %, the second natural frequency fell by almost 35 %, causing placement of the II-node, the 9th order critical in the immediate vicinity of the engine rated speed. In Figure 4 the crankshaft stress limits [23] are also included. The lower stress limit $\tau_1$ corresponds to the engine continuous running, while the upper stress limit $\tau_2$ is applicable to the engine transient operation only.

The crankshaft peak torque is most sensitive to the values of the tuning wheel and turning wheel mass moments of inertia change, as shown by 672 and 626 kN·m average changes, respectively. In addition, a significant sensitivity to the shafting stiffness is also present, where 570 kN·m average change is found. The crankshaft peak torque least sensitivity is found with respect to the propeller mass moment of inertia, where an average change of 341 kN·m is recorded.

### 4.3. Shafting peak torque

Where the six-cylinder two-stroke diesel propulsion plants are concerned, the shafting peak torque is exclusively induced by the main resonance of the plant, i.e. the I-node, 6th order critical, Figure 5. Figure 5 depicts the intermediate shaft stress levels for the two typical shafting arrangements, already defined in Section 4.2. With the exception of a narrow engine speed range characterised by the excessive torsional stresses, the remaining engine speed range is free of any harmful criticals.
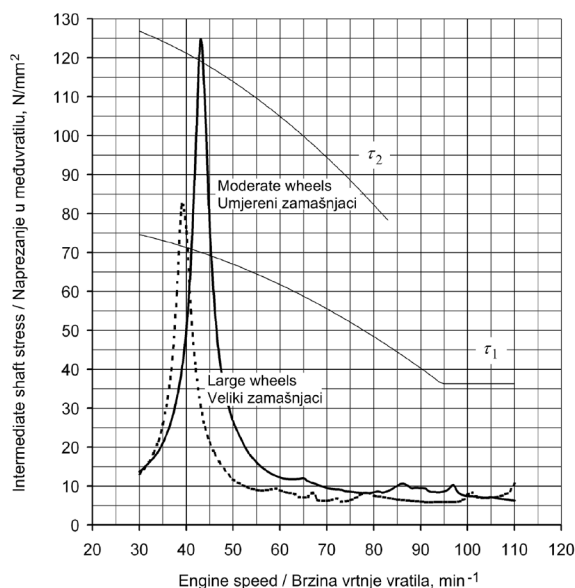


**Figure 5.** Typical intermediate shaft torsional vibration response

**Slika 5.** Tipični odziv torzijskih vibracija međuvratila

The values of the shafting peak torque within the screened design space, Figure 6, range between 1211 and 3674 kN·m. The least shafting torque corresponds to the least shafting stiffness and propeller mass moment of inertia, and the largest turning wheel and tuning wheel mass moments of inertia, Figure 6(g). The highest shafting torque corresponds to the highest shafting stiffness and propeller mass moment of inertia, and the least tuning wheel and turning wheel mass moments of inertia, Figure 6(d).

Figures 6(a)-(d) show the relationship between the shafting peak torque and turning wheel and tuning wheel mass moments of inertia. The relationship between the shafting peak torque and shafting stiffness and propeller inertia is provided in Figures 6(e)-(h). Similar to the natural frequency response surfaces, Figure 2, diagrams in both groups follow the same column-specific pattern. Besides, all response surfaces are smooth and monotone. Therefore, the extreme responses are always positioned on the design space boundaries.

The shafting peak torque is the most sensitive to the tuning wheel inertia, where a $\overline{\Delta}$ =746 kN·m average change is found. Nearly the same sensitivity is also recorded with respect to the shafting stiffness, where a $\overline{\Delta}$ =734 kN·m average change is calculated. Significantly lower sensitivities are found with respect to the propeller and turning wheel inertias, where an average change of 570 and 319 kN·m is calculated, respectively.

### 4.4. System parameter influence factors

System parameters concerned possess variable ability to change the analysed vibration responses. In order to quantify these abilities, Saaty's priority theory [24] has been applied. The priority theory is based on a pairwise comparison of the system parameters with respect to the considered criterion, e.g. mean response change, equation(8). Then, the parameters can be ranked by determining the normalized eigenvector **v** of the eigenvalue problem:

$$\mathbf{Rv} = \lambda \mathbf{v} , \tag{9}$$

where $\lambda$ is the only positive eigenvalue of a reciprocal comparison matrix **R**. Each element of **R** is defined by:

$$r_{ij} = \overline{\Delta}_i / \overline{\Delta}_j , \tag{10}$$

where both indices range from one to four, the number of parameters considered.

Table 3 provides values of the normalized eigenvectors **v**, multiplied by 100, with corresponding ranks (in parenthesis), for each of the considered vibration responses. The last column contains the system parameter overall influence factors. They are also determined by the approach of equation (9), but with newly defined elements of the reciprocal comparison matrix **R**:

$$r_{ij} = \frac{\sum\limits_{k} w_k \cdot v_{ik}}{\sum\limits_{k} w_k \cdot v_{jk}} , \tag{11}$$

where $k$ ranges from one to three, the number of vibration responses considered, and $w_k$ are the corresponding weights. In the present study the following weight factors were applied: 0,1 for natural frequency, 0,3 for crankshaft peak torque and 0,6 for shafting peak torque.

The results provided in Table 3 stress the dominant influence of the shafting stiffness on the propulsion shafting torsional vibration behaviour. They also imply a relatively weak influence of the turning wheel mass moment of inertia. Therefore, it could be concluded that it is usually more effective to add a tuning wheel instead of enlarging the already mounted turning wheel.
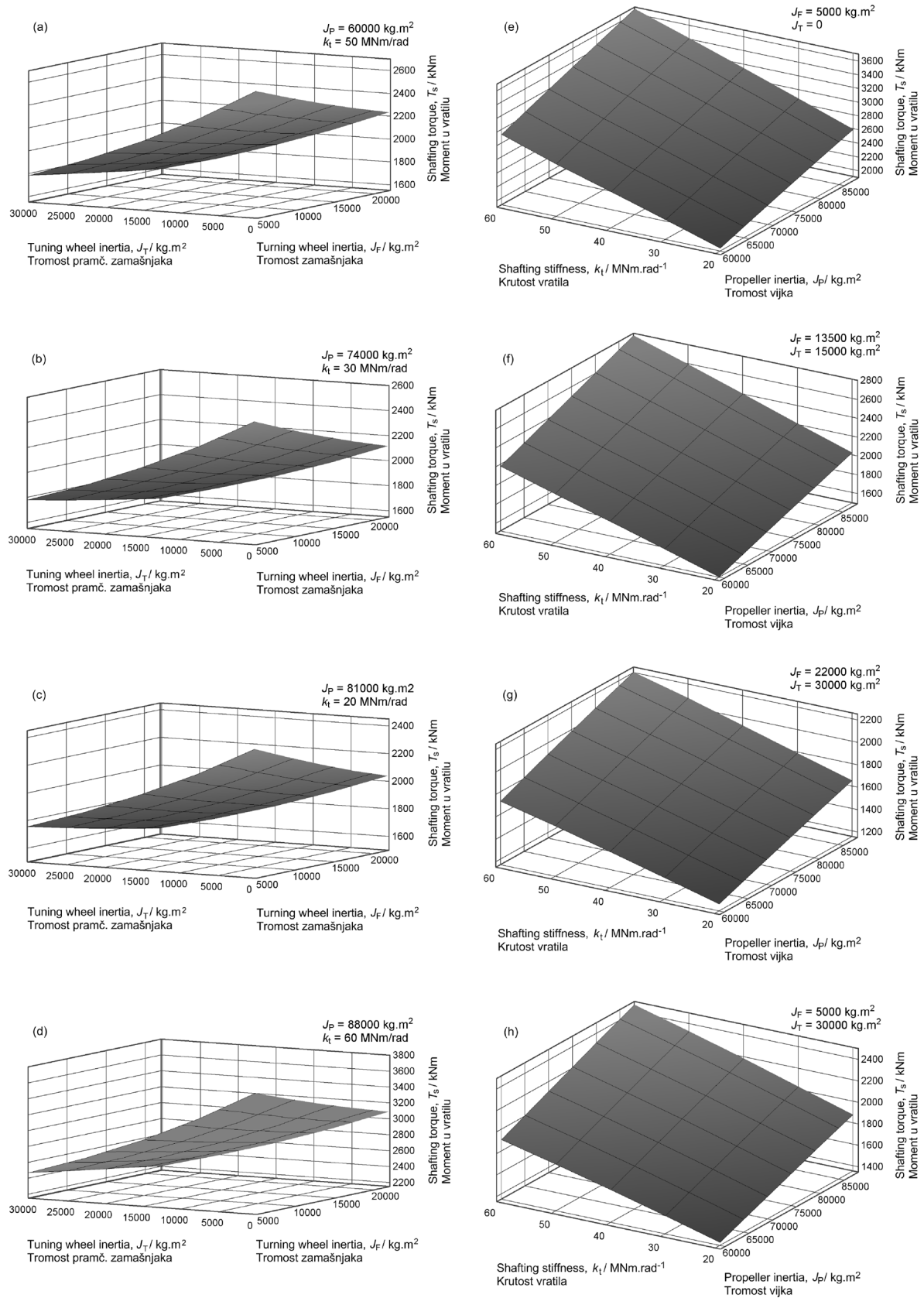
**Figure 6.** Shafting peak torque response surfaces

**Slika 6.** Odzivne plohe vršnoga torzijskog momenta u vodu vratila

**Table 3.** System parameter influential factors (normalised and multiplied by 100; values in parenthesis denote ranks)
**Tablica 3.** Faktori upliva parametara sustava (normirani i pomnoženi sa 100; vrijednosti u zagradama su rangovi)

| System parameter / Parametar sustava | Natural frequency / Prirodna frekvencija | Crankshaft peak torque / Vršni moment u koljenastom vratilu | Shafting peak torque / Vršni moment u vodu vratila | Overall / Ukupno |
|---|---|---|---|---|
| Shafting stiffness / Krutost vratila | 69,80 (1) | 25,80 (3) | 30,98 (2) | 33,30 (1) |
| Propeller inertia / Tromost vijka | 15,56 (2) | 15,44 (4) | 24,05 (3) | 20,62 (3) |
| Turning wheel inertia / Tromost zamašnjaka | 3,73 (4) | 28,32 (2) | 13,48 (4) | 16,96 (4) |
| Tuning wheel inertia / Tromost pramčanoga zamašnjaka | 10,91 (3) | 30,44 (1) | 31,49 (1) | 29,12 (2) |

## 5. Discussion

The considered design space, Table 2, makes up the majority of real-life propulsion shafting designs. During the study a much wider range of shafting stiffness was considered (up to 100 MN·m/rad). However, at a later stage, the shafting high stiffness area was dropped, due to two reasons. The first one is the clarity of presentation (response surfaces are smooth, monotone, and could be extrapolated by extending the ones provided in Figures 2, 3 and 6), and the second one is the inferior technical merits of the stiff shafting designs. The high-stiffness shafting designs are usually costly solutions; they introduce a harmful propeller variable thrust and, finally, introduce additional troubles during the shaft alignment process.

To simplify analysis, a complete shafting system consisting of intermediate shaft and a propeller shaft has been modelled as a two-mass system only, although it is customary modelled as at least the three-mass system. Fortunately, this simplification should not alter the results significantly, since the tests performed on a two real-life shafting arrangements have shown that the maximum response error is less than 1,4 %.

The present study did not take into account the possibility of substituting the tuning wheel by an appropriate torsional vibration damper. There are two reasons for such approach. First, introduction of the torsional vibration damper would significantly complicate the analysis, since the vibration damper almost doubles the number of system parameters. Second, it reflects the author's position that it is more cost-effective and technically justified to resolve the torsional vibration problems in a natural way, by system parameters adjustment, whenever possible.

## 6. Conclusions

The following conclusions can be drawn from the present study:

- Shafting stiffness has a major impact on the propulsion system forced torsional vibration amplitudes. In general, lower shafting stiffness and lower propeller mass moment of inertia provide more desirable torque and stress responses.

- Turning wheel and tuning wheel mass moments of inertia are additional designer's tools to obtain desired system responses. However, it should be clearly realized that large wheels in conjunction with the sufficiently flexible shafting could provoke an unacceptably high crankshaft torque and stress levels in the vicinity of the engine service speed.

- Large sensitivity indicators which were found suggest that there is usually a lot of room for the system response improvement. This is specifically true in the cases when two or more system parameters are adjusted simultaneously.

- The presented results provide a more thorough insight into the propulsion system torsional behaviour and encourage the designers to achieve a desired design solution already in the preliminary design phase.

- Although the key findings are related to the specific diesel engine only, it is believed that the presented behaviour is quite general and hence qualitatively applicable to a much broader range of the two-stroke slow speed diesel propulsion plants.

## Acknowledgement

## REFERENCES

[1] LONG, C. L.: *Propellers, shafting, and shafting system vibration analysis*, in: R. L. Harrington (ed.), Marine Engineering, Society of Naval Architects and Marine Engineers, Jersey City, 1992.

[2] LEHR, E.; PARKER, E. L.: *Considerations in the design of marine propulsion shaft systems*, Transactions of SNAME, 69 (1961), 555-601.

[3] MOTT, I. K.; FLEETING, R.: *Design aspects of marine propulsion shafting systems*, Transactions of IME, 79 (1967), 177-220.

[4] ...: *Vibration characteristics of two-stroke low speed diesel engines*, revised from P.8703-165, MAN B&W Diesel, Copenhagen, 1988.

[5] DAHLER, G.; ROALDSØY, J.; SANDBERG, E.: *Det Norske Veritas'methodology for propulsion shaft design - a cost saving and reliable supplement to the IACS simplified code*, Proceedings of the Symposium on propellers and shafting, Williamsburg, 2006.

[6] MAGAZINOVIĆ, G.: *Shaftline design considerations of five-cylinder low-speed propulsion plants*, Proceedings of the 13th Symposium on theory and practice of shipbuilding (SORTA 98), Zadar, 1998.

[7] MAGAZINOVIĆ, G.: *Utility of high-strength steels for main propulsion shafting design*, Proceedings of the IX congress (IMAM 2000), Ischia Porto, 2000.

[8] MAGAZINOVIĆ, G.: *Significance of shafting length: a Suezmax tanker design problem*, Proceedings of the 10th international congress (IMAM 2002), Rethymnon, 2002.

[9] SVERKO, D.: *Design considerations in propulsion shafting alignment*, Proceedings of the 9th ICMES conference, Helsinki, 2003.

[10] STOUFFS, R.: *Design spaces: the explicit representation of spaces of alternatives*, Artificial Intelligence for Engineering, Design, Analysis and Manufacturing, 20 (2006), 61-62.

[11] HASSENZAHL, M.; WESSLER, R.: *Capturing design space from a user perspective: the repertory grid technique revisited*, International Journal of Human-Computer Interaction, 12(2000), 441-459.

[12] MACLEAN, A.; YOUNG, R. M.; BELLOTTI, V. M. E.; et al.: *Questions, options, and criteria: elements of design space analysis*, International Journal of Human-Computer Interaction, 6 (1991), 201-250.

[13] KER WILSON, W.: *Practical Solution of Torsional Vibration Problems*, Vol. 1, Frequency Calculations, Chapman & Hall, London, 1956.

[14] NESTORIDES, E. J.: *A Handbook on Torsional Vibration*, Cambridge University Press, London, 1958.

[15] WU, J-S.; CHEN, W-H.: *Computer method for forced torsional vibration of propulsive shafting system of marine engine with or without damping*, Journal of Ship Research, 26 (1982), 176-189.

[16] AKAZAWA, M.; HONDA, M.: *Torsional vibration in geared diesel system*, Japan Shipbuilding & Marine Engineering, 3 (1968) 6, 23-33.

[17] HAFNER, K. E.; MAASS, H.: *Theorie der Triebwerksschwingungen der Verbrennungskraftmaschine*, Springer Verlag, Wien, 1984.

[18] HAFNER, K. E.; MAASS, H.: *Torsionsschwingungen in der Verbrennungskraftmaschine*, Springer Verlag, Wien, 1985.

[19] WALKER, D. N.: *Torsional Vibration of Turbomachinery*, McGraw-Hill, New York, 2003.

[20] PARSONS, M. G.: *Mode coupling in torsional and longitudinal shafting vibrations*, Marine Technology, 20 (1983) 3, 257-271.

[21] MAGAZINOVIĆ, G.: *TorViC v1.1 – Program for Propulsion System Torsional Vibration Analysis: User's Guide*, CADEA, Split, 2000 (in Croatian).

[22] ...: *Dimensions of propulsion shafts and their permissible torsional vibration stresses*, UR M68, International Association of Classification Societies, London, 2005.

[23] ...: *Calculation of crankshafts for I.C. engines*, UR M53, rev. 1, International Association of Classification Societies, London, 2004.

[24] SAATY, T. L.: *A scaling method for priorities in hierarchical structures*, Journal of Mathematical Psychology, 15 (1977), 234-281.